DEUTSCHES ELEKTRONEN-SYNCHROTRON DESY

DESY 86-154
December 1986

INVESTIGATION OF ONE- AND TWO-DIMENSIONAL QUANTUM SPIN SYSTEMS FOR MONTE CARLO SIMULATIONS

by

M. Marcu

II. Institut f. Theoretische Physik, Universität Hamburg

ISSN 0418-9833

NOTKESTRASSE 85 · 2 HAMBURG 52

To be sure that your preprints are promptly included in the
HIGH ENERGY PHYSICS INDEX ,
send them to the following address (if possible by air mail) :

DESY
Bibliothek
Notkestrasse 85
2 Hamburg 52
Germany

DESY 86-154
December 1986

ISSN 0418-9833

Investigation of One- and Two-Dimensional Quantum Spin Systems by Monte Carlo Simulations*

Mihail Marcu

II. Institut fuer Theoretische Physik
Universitaet Hamburg
Luruper Chaussee 149
2000 Hamburg 50, West Germany

Abstract: A method for simulating quantum spin systems with nearest neighbour interaction is reviewed. In the framework of a path-integral approach based on the Trotter formula, the quantum spin system is mapped into the limit of a sequence of classical spin systems with one extra dimension. Numerical questions connected to this limit are discussed. The role of particle and winding numbers is clarified. An overview of the problems investigated by our group is given. In particular, two new results are presented. A simulation of the one-dimensional spin S isotropic Heisenberg antiferromagnet, S=1/2, 1, 3/2, 2, supports Haldane's conjecture that the mass gap is zero for half-integer S and nonzero for integer S. For the two-dimensional spin 1/2 xy model we discuss evidence for a Kosterlitz-Thouless transition. In particular, we show that the helicity modulus can be computed directly from our simulaton.

1. Introduction

Since the pioneering work of Suzuki [1] there have been numerous attempts to simulate quantum spin systems using a path-integral approach (see [2,3] for reviews).

We consider for simplicity the Hamiltonian

$$H_\Lambda = -\sum_{<j,k>} (J_x S_j^x S_k^x + J_y S_j^y S_k^y + J_z S_j^z S_k^z + \vec{h}\cdot\vec{S}) \qquad (1.1)$$

Here $<j,k>$ is a nearest neighbour pair of lattice sites, S_j^α ($\alpha=x,y,z$) are spin S generators of SU(2) at the site j, J_α are couplings and $\vec{h}$ is an external magnetic field. The lattice will be denoted by Λ, $|\Lambda|=L$ in d=1 dimensions, $|\Lambda|=L_1 \times L_2$ in d=2, L, L_1 and L_2 are even. Periodic boundary conditions are assumed.

The expectation value of an operator O is defined by taking the thermodynamic limit:

$$<O_\Lambda>_\Lambda = \frac{\mathrm{Tr}\ O_\Lambda \exp(-\beta H_\Lambda)}{\mathrm{Tr}\exp(-\beta H_\Lambda)} \xrightarrow[\Lambda\to\infty]{} <O> \qquad (1.2)$$

(β is the inverse of the temperature T). Notice that O_Λ is not necessarily equal to O, only $O_\Lambda \to O$ is required. Now we decompose H_Λ into sums over commuting local operators K(r)

$$H_\Lambda = -A_\Lambda - B_\Lambda\ ,\quad A_\Lambda = \sum_{r\in S_1} K(r)\ ,\quad B_\Lambda = \sum_{r\in S_2} K(r) \qquad (1.3)$$

* Talk given at the "Taniguchi Symposium on Quantum Monte Carlo Simulations", Shizuoka, Japan, November 1986

$S_{1,2}$ being two sublattices, and we use the Trotter formula [4]

$$\exp(-\beta H_\Lambda) = \lim (T_{\Lambda,M})^{M/2} \quad , \quad T_{\Lambda,M} = \exp(\bar{\beta} A_\Lambda) \exp(2\bar{\beta} B_\Lambda) \exp(\bar{\beta} A_\Lambda) \qquad (1.4)$$

with $\bar{\beta}=\beta/M$, M=even. The expectation value $\langle O_\Lambda \rangle_\Lambda$ is obtained as the limit

$$\langle O_{\Lambda,M} \rangle_{\Lambda,M} = \frac{\mathrm{Tr}\, O_{\Lambda,M} (T_{\Lambda,M})^{M/2}}{\mathrm{Tr}\, (T_{\Lambda,M})^{M/2}} \xrightarrow[M\to\infty]{} \langle O_\Lambda \rangle_\Lambda \qquad (1,5)$$

Again, $O_{\Lambda,M}$ is in general different from O_Λ, but $O_{\Lambda,M} \to O_\Lambda$ as $M\to\infty$. By inserting complete sets of eigenstates of the S_j^α operators, α = z or x, a classical spin system on the lattice ΛxM is obtained. For $\vec{h}=0$, this system will have constraints [5]. In particular, if we use z-spins as intermediate states the configurations can be interpreted as sets of particle world lines [6-8] (in [6] a preliminary account of our work was given).

In section 2 the classical spin system in d+1 dimensions (d=1,2) is discussed. The Monte Carlo procedure used to simulate it can update also the particle and winding numbers of the world lines. Section 3 deals with the numerical problems encountered when taking the $M\to\infty$ limit and the thermodynamic limit. In section 4 questions related to the particle and winding numbers are discussed. The conclusion is that the finite size effects are smaller if the particle number is allowed to vary but the winding number is fixed to zero. If we allow the winding number to vary, then in d=1 it turns out that in the thrmodynamic limit the winding number only takes the value zero. In d=2 this is true at high temperatures only. At low temperatures the winding number has a smooth distribution.

We have used our quantum Monte Carlo method to investigate a variety of models. In [8] we started to develop the method. For the first time a model with S>1/2 was simulated. In [9] the continuum limit of the Thirring model with Susskind Fermions was investigated. The first high precision quantum Monte Carlo simulation was performed in [10] for the d=1 S=1/2 isotropic ferromagnet and antiferromagnet. Our original analysis of the data in [10] was incorrect, as shown by comparison to Bethe-Ansatz results for the ferromagnet [11]. The reason was, paradoxically, that our low temperature data had too small statistical errors, so that the method we had previously used to extrapolate to the $M=\infty$ limit no longer worked. In [12] we showed that the discrepancies to [11] disappear when the extrapolation is done more carefully.

In order to perform high precision calculations, we wrote fully vectorized programs for general spin S in d=1 [13] and for S=1/2 in d=2. Further savings in computer time can be achieved using a variance reduction technique for quantum spin systems [14].

One-dimensional quantum spin systems have been studied in numerous experiments [15]. Typically the spin and coupling constants of some quasi-one-dimensional material are determined by some fairly reliable method (e.g. ESR) and then neutron scattering is studied. One difficulty in comparing theory with experiment is the lack of a reliable low-temperature approximation method. In [16] we showed for several S=1/2 and S=1 examples that quantum Monte Carlo results compare well to experiment in cases where other theoretical methods have failed.

Haldane [17] gave arguments that the S=∞ limit of d=1 xxz models is approached in a different way by integer and half-integer values of the spin S. In particular, he predicted that for the isotropic antiferromagnet the mass gap is zero for half-integer S and nonzero for integer S. This "Haldane conjecture" gave rise to a considerable controversy in the literature[18]. On the balance, S>1/2 finite chain diagonalization results seem to confirm the Haldane conjecture. Doubts remain however since the size of the chains for which exact diagonalization is still feasible is quite small. In section 5 we present results for S=1/2, 1, 3/2 and 2. They were obtained at finite temperatures for chains large enough to be effectively in the thermodynamic limit. The T→0 behaviour strongly supports the Haldane conjecture.

In two dimensions, the S=1/2 xy model (J_z=0) has also been subject to some controversy. The results of two calculations using different quantum Monte Carlo methods [19,20] do not agree [21]. In particular, the procedure of [19] is criticized for not being ergodic [21]. In section 6 we describe our preliminary results for the d=2 S=1/2 xy model. We establish a connection between the winding number distribution and the helicity modulus. At low temperatures our simulation yields a well-defined value for the helicity modulus. This is strong evidence for a massless phase [22] (i.e. a phase with power law decay of correlations). The possible interpretation of this result as evidence for a Kosterlitz-Thouless transition [23] is discussed. The acceptance rate for the update of the winding numbers in extremely small, and it decreases with increasing lattice size. Moreover, a simulation with variable winding numbers produces larger finite size effects than for fixed winding numbers. We indicate a way to compute the helicity modulus from fixed-winding-number simulations.

Section 7 contains our conclusions and outlook.

2. The Classical Spin System and the Monte Carlo Algorithm

In order to map the d-dimensional quantum spin system into a d+1-dimensional classical spin system, we used the following break-up of the Hamiltonian (see (1.3)):

$$\text{d=1:}\quad A_\Lambda = \sum_{j=\text{odd}} H(j,j+1)\ ,\quad B_\Lambda = \sum_{j=\text{even}} H(j,j+1) \tag{2.1.a}$$

$$\text{d=2:}\quad A_\Lambda = \sum_{j_1,j_2=\text{odd}} K(p_j),\quad B_\Lambda = \sum_{j_1,j_2=\text{even}} K(p_j)\ ,\quad j=(j_1,j_2) \tag{2.1.b}$$

$$\text{with } K(p_j) = H(j,j+\hat{1})+H(j+\hat{1},j+\hat{1}+\hat{2})+H(j+\hat{2},j+\hat{1}+\hat{2})+H(j,j+\hat{2})$$

Here H(j,k) is the link term in (1.1), $\hat{1}$, $\hat{2}$ are lattice unit vectors in direction 1, 2 (the lattice spacing is one), and $K(p_j)$ is the sum over the 4 link terms around the plaquette p_j (with lower left corner j). By inserting complete sets of eigenstates of S_j^z in (1.5), a classical spin system on the lattice Λ x M is obtained. A classical spin configuration s consists of spins s(j,r), jεΛ, r=1,...,M and s(j,r)ε{-S,-S+1,...,S-1,S}. The partition function is [1, 5, 7,6,8,20]:

$$\text{d=1:}\quad Z_{\Lambda,M} = \sum_s \prod_{p=\text{int}} f(p) \tag{2.2.a}$$

$$\text{d=2:}\quad Z_{\Lambda,M} = \sum_s \prod_{c=\text{int}} f(c) \tag{2.2.b}$$

Here p=int means an interacting plaquette in 1+1 dimensions, c=int an interacting cube in 2+1 dimensions. For p=int the coordinates of the lower-left corner are both even or both odd. For c=int the coordinates of the lower-left-forward corner are all three even or all odd (there are LM/2 interacting plaquettes and $L_1L_2M/4$ interacting cubes). With the notation introduced in fig.1, the contribution of an interacting plaquette or cube to the Boltzmann weight of a configuration is:

$$d=1: \quad f(p) = \langle s_1,s_2|\exp\{-2\tilde{\beta}H(j,j+1)\}|s_1',s_2'\rangle \tag{2.3.a}$$

$$d=2: \quad f(c) = \langle s_1,s_2,s_3,s_4|\exp\{-2\tilde{\beta}K(p_j)\}|s_1',s_2',s_3',s_4'\rangle \tag{2.3.b}$$

As a consequence of the symmetries of (1.1), the configurations of the classical spin system may be subject to constraints. For the xxz model, defined by $J_x=J_y$, $\vec{h}=0$ (or $\vec{h}$ in z-direction) the total magnetization in z-direction $S^z_{tot} = \Sigma\, S^z_j$ is conserved and f is zero unless (xxz constraint):

$$d=1: \quad s_1+s_2 = s_1'+s_2' \tag{2.4.a}$$

$$d=2: \quad s_1+s_2+s_3+s_4 = s_1'+s_2'+s_3'+s_4' \tag{2.4.b}$$

For the xyz model, defined by $\vec{h}=0$ (or $\vec{h}$ in z-direction) the total magnetization is conserved only modulo 2, and eqs.(2.4) hold modulo 2 (xyz constraint). The other symmetries do not lead to constraints, but to symmetries of f. Thus in d=2 f is invariant under the group D_{4h}.

For the xxz model (2.4) implies:

$$n_p = \sum_{j\in\Lambda} s(j,r) = \text{constant in } r \tag{2.5}$$

A configuration can be seen as a set of particle lines. There are s(j,r)+S world lines of particles passing through the point j,r of Λ x M. The particle lines wind around the torus both in Trotter (Euclidean time) and in space directions [7,6,8]. The conserved total number of perticle lines is $n_p+|\Lambda|S$. Eqs.(2.4) also imply conservation of the winding number(s) n_w [8,25]:

$$d=1: \quad n_w = \sum_r (-1)^{j+r} s(j,r) = \text{constant in } j \tag{2.6.a}$$

$$d=2: \quad n_{w_1} = \sum_{j_2,r} (-1)^{j_1+r} s(j,r) = \text{constant in } j_1\ ,\ \ j=(j_1,j_2) \tag{2.6.b}$$

and n_{w_2} is defined similarly, by interchanging j_1 and j_2.

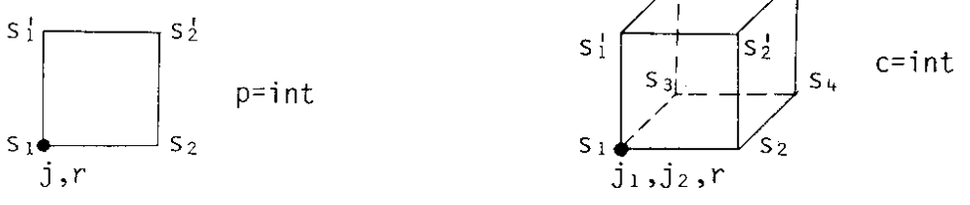

Fig.1: An interacting plaquette (j,r = even or j,r = odd) and an interacting cube (j_1,j_2,r = even or j_1,j_2,r=odd).

For the xyz model the particle and winding numbers are conserved only modulo 2.

The existence of constraints restrict the class of expectation values (1.2) that can be computed using (1.5) [8-10]. The general rule is that $O_{\Lambda,M}$ is a product of S^z_j operators or is obtained by taking derivatives of the free energy of the classical system on $\Lambda \times M$. Sometimes other quantities are also accessible. In order to compute x-x correlations however, a new simulation with J_x and J_z interchanged has to be performed. As will be discussed later, all these quantities can be computed both for fixed and for variable particle and winding numbers.

Let us now describe the Monte Carlo algorithm used to simulate the xxz model. There are three different updating procedures: a local update that preserves the values of n_p and n_w, an update of n_p and an update of n_w.

In 1+1 dimensions the local update changes the values of the 4 spins at the corners of a noninteracting plaquette. In the notation of fig.2:

$$s_1 \to s_1+\sigma \ , \quad s_2 \to s_2-\sigma \ , \quad s_3 \to s_3+\sigma \ , \quad s_4 \to s_4-\sigma \ , \ \sigma = \pm 1 \qquad (2.7)$$

The constraint (2.4.a) is not violated for any of the 4 neighbouring interacting plaquettes. In 2+1 dimensions the local update involves 4-spin changes for the plaquettes that are not on the boundary of some interacting cube. If such a plaquette is time-like, then (2.7) is used for the update; if it is space-like, then the 4-spin change is:

$$s_1 \to s_1+\sigma \ , \quad s_2 \to s_2-\sigma \ , \quad s_3 \to s_3-\sigma \ , \quad s_4 \to s_4+\sigma \ , \ \sigma = \pm 1 \qquad (2.8)$$

The constraint (2.4.b) is not violated for any of the 4 neighbouring interacting cubes. In 1+1 dimensions (2.7) can "deform" a particle line locally in all directions. This is not true however in 2+1 dimensions. In this case we supplement the local update procedure by offering changes that result from the formal product of two one-plaquette changes (2.7)-(2.8), such that the two plaquettes are faces of the same noninteracting cube. It may happen that a single plaquette-change leads to a zero weight (i.e. not allowed) configuration, but a formal product of two such changes again produces a configuration with nonzero weight. Using this local update procedure, a particle line in 2+1 dimensions can be also locally deformed in all directions [25].

Notice that for S=1/2 eqs.(2.7)-(2.8) can be replaced by a simple flip of all 4 spins.

The particle number update is performed by offering:

$$s(j,r) \to s(j,r)+\sigma \ , \ \sigma = \pm 1 \ , \quad \text{for all } r=1,\ldots,M \qquad (2.9)$$

This ammounts to inserting or removing a straight particle line. The winding number is updated by (update of n_w and n_{w_1}):

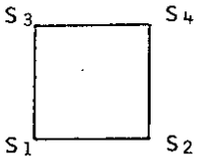

Fig.2: Notation for the 4-spin changes (2.7)-(2.8)

$$d=1: \quad s(j,r) \to s(j,r)+ (-1)^{j+r}, \ \sigma = \pm 1 \ , \quad \text{for all } j=1,\ldots,L \qquad (2.10.a)$$

$$d=2: \quad s(j,r) \to s(j,r)+ (-1)^{j_1+r}, \ \sigma = \pm 1 \ , \quad j = (j_1,j_2) \ , \quad \text{for all } j_1=1,\ldots,L_1 \qquad (2.10.b)$$

Interchanging j_1 and j_2 in (2.10.b) we get the update of n_{W_2}.

For the xyz model, the local update is supplemented by offering a one-spin change:

$$s(j,r) \to s(j,r)+\sigma \ , \quad \sigma = \pm 2 \qquad (2.11)$$

For S=1/2 this is not necessary.

In 1+1 dimensions (2.7)-(2.10) define an ergodic Markov process for the xxz model. Unfortunately we could not proove that this is true also in 2+1 dimensions. However, since the particle lines can be deformed locally in all directions (if 2-plaquette changes are included), we are confident that (2.7)-(2.10) define an ergodic process in this case too.

Eqs. (2.9)-(2.11) define an ergodic Markov process for the xyz model, both in 1+1 and in 2+1 dimensions.

In section 4 it will be argued that the nonlocal parts (2.9)-(2.10) of the Monte Carlo algorithm can be dropped sometimes. Furthermore it will be shown that an optimal procedure is to update n_p but to keep $n_W=0$. This is extremely important in view of the typically very small acceptance rate for (2.10) [8, 25 ,26]. The acceptance rate for the local and the particle number update is usually reasonable.

3. Problems Concerning the $M \to \infty$ and the Thermodynamic Limits

It was noticed by several workers that the linear correction in 1/M to the $M \to \infty$ limit vanishes (see [2,3] for reviews). In particular, in refs. [8-10] we observed that

$$\langle O_{\Lambda,M}\rangle_{\Lambda,M} = \langle O_\Lambda\rangle_\Lambda + \bar{\beta}^2 \, \beta \sum_{j\in\Lambda} (\langle OB_j\rangle_\Lambda - \langle O\rangle_\Lambda \langle B_j\rangle_\Lambda) + \ldots \qquad (3.1)$$

where B_j are local operators obtained from double commutators of A_Λ and B_Λ.

Suzuki [27] gave a one-line proof that the r.h.s of (3.1), considered as a function of $\bar{\beta}$ ($\bar{\beta}=\beta/M$) and β, is even in $\bar{\beta}$ (one must be careful not to introduce odd powers of $\bar{\beta}$ by an unhappy choice of $O_{\Lambda,M}$).

As $T \to 0$ one has to take larger values of M in order to be numerically close to the $M \to \infty$ limit. In [7] it was argued that the size of the corrections to the $M \to \infty$ limit only depends on the value of $\bar{\beta}$. Our investigations however [8-10,12,16,25,26,28] do not confirm this as a general rule. In the important case that T=0 is a critical point, the coefficients in front of the even powers of $\bar{\beta}$ (see (3.1)) sometimes have a nonnegligible dependence on β, and they may behave differently for different physical quantities.

At the beginning [8,10] we extrapolated to the $M \to \infty$ limit by taking values of M high enough such that the r.h.s. of (3.1) was effectively linear in $\bar{\beta}$. This is however very dangerous, as discussed in [12,26]. A correct procedure is to fit (3.1) with polinomyals in $\bar{\beta}^2$ whose order is increased until the extrapolated result stabilizes. The fits must be done for every quantity for every temperature and for every set of coupling constants separately, and goodness-of-fit tests should not be ommited.

Suzuki argued that the thermodynamic limit $\Lambda \to \infty$ and the "Trotter limit" $M \to \infty$ can be interchanged [29]. His proof however does not seem to hold for the systems (2.2) that interest us here. In [12,26] we checked numerically that the two limits can indeed be interchanged. For various one-dimensional xxz models we compared the results obtained by first taking the $M \to \infty$ limit and then the $L \to \infty$ limit with those obtained by taking the $M = L \to \infty$ limit. Within errorbars they were always the same.

4. Role of Particle and Winding Numbers in xxz Models

In [7] it was argued that, similarly to the equivalence of canonical and grand-canonical ensembles in the thermodynamic limit, the expectation values of local oprators should not depend on particle and winding numbers:

$$\lim_{\Lambda\to\infty} \lim_{M\to\infty} \langle O_{\Lambda,M} \rangle_{\Lambda,M,n_p=n,n_w=w} = \text{independent of } n \text{ and } w \qquad (4.1)$$

As far as particle number is concerned, the idea for a proof can be found in many Statistical Mechanics textbooks. Let us discuss the reason why we do not expect (4.1) to depend on w . The winding number is defined by counting the particle lines that go around the torus in space directions. Therefore, fixed and variable winding numbers should correspond to different types of boundary conditions. In the thermodynamic limit the boundary conditions should play no role.

In a Monte Carlo simulation the problem of finite size effects is very important. In general, finite size effects are smaller if we use a grand-canonical ensemble. Thus in a simulation with variable particle number the thermodynamic limit is approached faster than in the case of fixed particle number. Moreover, we are often interested in nonlocal quantities (e.g. susceptibility) that cannot be computed if the particle number is not allowed to vary [8,10,21].

Let us discuss the shape of the particle and winding number distributions

$$\rho_p(n) = \langle \delta(n_p - n) \rangle \ , \quad \rho_w(w) = \langle \delta(n_w - w) \rangle \qquad (4.2)$$

(δ is the Kronecker symbol). In all the models we have studied, $\rho_p(n)$ is a smooth curve, even in the thermodynamic limit. If at T=0 there is no z-magnetization, the peak at n=0 becomes narrower with decreasing temperature. If we are interested in obtaining T=0 results, it might be useful to keep the particle number n_p=0 [9,10]. If at T=0 the spontaneous magnetization is nonzero, then $\rho_p(n)$ broadens and tends to a constant as $T \to 0$ [8]. The winding number distribution behaves differently. In one-dimensional systems we find the following behaviour [12,26]. In a finite volume, $\rho_w(w)$ will be of course a

a smooth curve. As the volume is increased however, $\rho_w(w) \to \delta(w)$. Thus it is to be expected that simulations with $n_w=0$ give smaller finite size effects than in the case of variable winding number.

For the one-dimensional xy model ($J_x=J_y$, $J_z=\vec{h}=0$), we confirmed this conclusion using exact solutions [12]. Notice that the $n_w=0$ exact solution was obtained by diagonalizing the transfer matrix in space (as opposed to the usual transfer matrix in Euclidean time) direction. The original winding number was mapped into the particle number of this new transfer matrix [26]. Monte Carlo simulations for $J_z\neq 0$ (d=1) also confirmed the fact that the finite size effects are smaller for $n_w=0$.

In the two-dimensional xy model we found a different picture for the winding number distribution. The model has a phase transition at finite temperatures. In the high-T phase we found again that $\rho_w(w) \to \delta(w)$ in the thermodynamic limit. In the low-T phase however, $\rho_w(w)$ seems to converge towards a smooth curve [25]. Nevertheless, at all temperatures the finite size effects are smaller for $n_w=0$ than for variable winding number.

In section 6 a connection between $\rho_w(w)$ and the helicity modulus will be established. This is in agreement to our general statement that different winding numbers mean different boundary conditions.

We conclude this section by restating our main conclusion: the most efficient simulation of an xxz system is with variable n_p and with $n_w=0$. Fixed n_p is useful if we study T=0 properties and there is no magnetization at T=0. Variable n_w is useful in computing the helicity modulus, although in section 6 a fixed n_w method will be also proposed.

5. Quantum Monte Carlo Test of the Haldane Conjecture

We performed a high precision calculation for the d=1 isotropic antiferromagnet with S = 1/2, 1, 3/2, 2 [28]. In order to extrapolate to the thermodynamic and $M \to \infty$ limits, the largest lattices we took were L=M=120.

If there is a mas gap, the S^z-S^z correlation function should decay exponentially even in the limit T=0. Its Fourier transform, the static structure factor I(q), will, in a small region around the peak at $q=\pi$, converge towards a Lorentzian curve as $T \to 0$. If on the other hand at T=0 we have a power-law decay of the correlation function, then $I(\pi)$ will diverge as $T \to 0$.

In fig.3 we present our results for $I(\pi)$ as a function of temperature. The behaviour is very different for S = 1/2 and 3/2 as compared to S = 1 and 2. If $I(\pi)$ diverges we have a power-law approach to T=0

$$I(\pi) \sim T^{-\gamma_1} \tag{5.1}$$

and in fig.3 we should get a straight line with slope γ_1. For S = 1 and 2 this is evidently not the case. For S = 1/2 and 3/2 a fit with a straight line is possible, giving the values $\gamma_1=.22\pm.03$ for S=1/2 and $\gamma_1=.70\pm.05$ for S=3/2. For S=1/2 it is known that $\gamma_1=0$ and that $I(\pi)$ diverges as the logarithm of T (see [7] and references therein). This is not inconsistent with our data since it is very difficult to distinguish between a small power and a log.

We also computed the staggered susceptibility, which in the case of

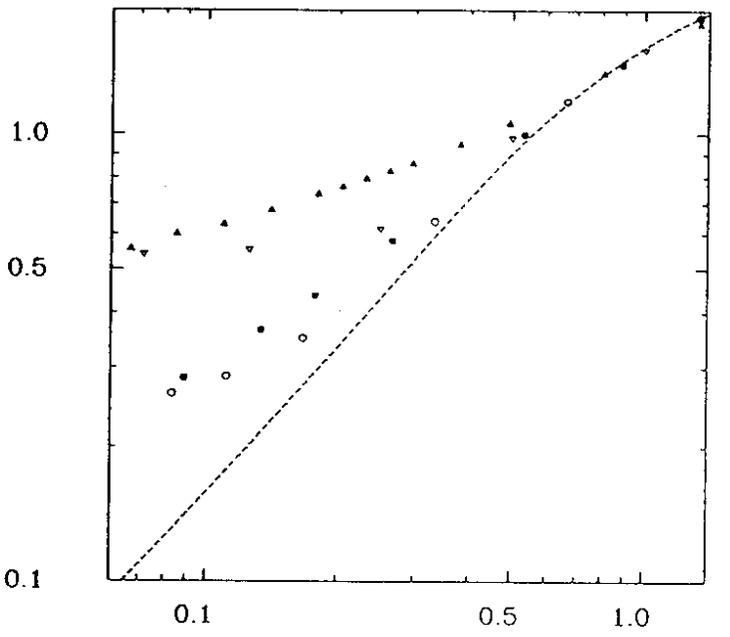

Fig.3 Log-log plot of $[I(\pi)/S(S+1)]^{-1}$ against $T/S(S+1)$. The full triangles are S=1/2, the empty triangles are S=1, the full squares are S=3/2, and the empty circles are S=2. The dashed line is the S=∞ limit.

zero mass gap should diverge with the exponent $\gamma=\gamma_1+1$ [30]. An analysis similar to that for $I(\pi)$ gave the result $\gamma=1.05\pm.06$ for S=1/2 and $\gamma=1.70\pm.06$ for S=3/2.

From our data it seems that for half-integer spins the exponent γ_1 grows from 0 to 1 as S increases from S=1/2 to S=∞ (γ goes from 1 to 2). In [31] however, it is argued that $\gamma_1=0$ for all finite half-integer S. For S>1/2 this would mean that at very low T there is a crossover from γ_1 close to 1 to $\gamma_1=0$. In the S=∞ limit the crossover temperature would go to zero. It is not clear whether a quantum Monte Carlo simulation could decide which alternative is correct.

6. The Two-Dimensional Spin 1/2 xy Model

For this model we performed two simulations, one with variable winding number and one with $n_w=0$. The behaviour of the winding number distribution and of the finite size effects was discussed in section 4. Here a connection between $\rho_w(w)$ and the helicity modulus will be established.

In the classical case, the helicity modulus was defined in [22]. Consider the partition function $Z(\theta)$ with a twist of θ in the angle variables across the boundary in 1-direction. Then [22]

$$\frac{Z(\theta)}{Z(0)} \underset{\theta/L_1=\text{small}}{=} \exp(-\theta^2 \beta T L_2/2L_1) \qquad (6.1)$$

T is called helicity modulus . In the low temperature phase we expect a non-zero value of T, while for $T>T_c$ T=0 in the thermodynamic limit. Notice that (6.1) depends very sensitively on the values of L_1 and L_2.

For the quantum xxz model we define the twisted boundary conditions by changing the Hamiltonian across the boundary as follows:

$$H(j,j+\hat{1}) \to \exp(i\theta S^z_j)\, H(j,j+\hat{1})\, \exp(-i\theta S^z_j)\ , \quad j=(j_1,j_2)\ ,\ j_1=L_1 \quad j_2=1,\ldots,L_2 \tag{6.2}$$

It is easily seen that for $S \to \infty$ the correct twisted boundary conditions are obtained. The path-integral method described in sections 1 and 2 immediately leads to:

$$\frac{Z(\theta)}{Z(0)} = \langle \exp(i\theta n_w) \rangle = \sum_w \exp(i\theta w)\ \rho_w(w) \tag{6.3}$$

$Z(\theta)/Z(0)$ can thus be computed directly in a simulation with variable winding number, and it is the Fourier transform of $\rho_w(w)$.

In the low temperature region we could fit our data well with the form (6.1) for 4 x 4, 4 x 8, 8 x 4 and 8 x 8 lattices (the highest value of M was 32). This strongly suggests that $T \neq 0$ for $T<T_c$ and therefore the low-T phase is massless [25].

We interpret this as evidence for a Kosterlitz-Thouless phase transition [23], i.e. a transition from a massive to a massless phase such that the correlation length blows up exponentially as $T \to T_c$, $T>T_c$, and such that there is no symmetry breaking for $T<T_c$. Other groups have also found evidence for a massless phase at $T<T_c$ [20,32]. However, in [19] it is argued that for $T>T_c$ the data show a power-law divergence of the correlation length. No model is known in the literature where this $T>T_c$ behaviour is combined with the Kosterlitz-Thouless behaviour for $T<T_c$. It is therefore very important to do further investigations.

Notice that if we take $\theta=\pi$ in (6.3), only the winding number modulo 2 is important. Then the formula holds also for the xyz model.

Because of a very low acceptance rate, it is very difficult to compute T for large lattices using (6.3). Manipulating (6.3) it can be shown that the difference between the energies for $n_w=1$ and $n_w=0$ is a numerically simple function of T. Using this method, the helicity modulus could be computed for much larger lattices.

7. Conclusions and Outlook

In this paper the quantum Monte Carlo work done by our group has been reviewed. In particular, we discussed the various limits carefully, as well as the problems connected to the particle and winding numbers. We argued that it is safe and even desirable to keep the winding number zero.

In a high precision simulation we gave strong numerical evidence for the validity of the Haldane conjecture. For the d=2 S=1/2 xy model we computed the helicity modulus as the Fourier transform of the winding number distribution.

The work on the Haldane conjecture will be continued in order to see how the $S=\infty$ limit is approached for half-integer spins. Our main effort in the near future will be in d=2, in the investigation of the S=1/2 xxz model.

References

1. M.Suzuki: Commun.Math.Phys.51 (1976) 183
   Prog.Theor.Phys.56 (1976) 1454
   M.Suzuki, S.Miyashita and A.Kuroda: Prog.Theor.Phys.58 (1977) 1377
2. M.Suzuki: J.Stat.Phys.43 (1986) 883
3. H.de Raedt and A.Lagendijk: Phys.Repts.127 (1985) 223
4. H.F.Trotter: Proc.Am.Math.Soc.10 (1959) 545.
5. M.Barma and B.Shastry: Phys.Rev.B18 (1978) 3351
6. J.Honerkamp: In "Recent Advances in Field Theories and Statistical Mechanichs", Les Houches 1982, eds. J.-B.Zuber and R.Stora (Elsevier Science Publishers B.V., 1984) p.248
7. J.E.Hirsch et.al.: Phys.Rev.Lett.47 (1981) 1628; Phys.Rev.B26 (1982) 5033
8. M.Marcu and A.Wiesler: J.Phys.A18 (1985) 2479
9. F.-K.Schmatzer: "Massenberechnungen am Massiven Thirringmodell mit Hilfe der Monte Carlo Methode", Diplomarbeit, Freiburg 1983
10. M.Marcu, J.Mueller and F.-K.Schmatzer: J.Phys.A18 (1985) 3189
11. P.Schlottmann: Phys.Rev.Lett.54 (1985) 2131
    M.Takahashi and M.Yamada: J.Phys.Soc.Japan 54 (1985) 2808
12. M.Marcu, J.Mueller and F.-K.Schmatzer: Phys.Lett.116A (1986) 447
13. M.Marcu, J.Mueller and F.-K.Schmatzer: "Fast Algorithm for One-Dimensional Quantum Monte Carlo Simulations", Freiburg preprint THEP 86/6, submitted to Computer Phys.Comm.
14. M.Marcu and J.Mueller: "Variance Reduction Technique for Quantum Monte Carlo Simulations", Freiburg preprint THEP 86/7, to appear in Phys.Lett.A
15. L.J.de Jongh and A.R.Miedema: Adv.Phys.23 (1974) 1
    M.Steiner, J.Villain and C.G.Windsor: Adv.Phys.25 (1976) 87
16. M.Marcu and J.Mueller: "Quantum Monte Carlo versus Experimental Results for xxz Chains", Freiburg preprint THEP 86/8, submitted to Phys.Lett.A
17. F.D.M.Haldane: Phys.Rev.Lett.50 (1983) 1153; Phys.Lett.93A (1983) 464
18. R.Botet and R.Julien: Phys.Rev.B27 (1983) 613
    M.Kolb, R.Botet and R.Julien: J.Phys.A16 (1983) L673
    J.B.Parkinson et.al.: J.Appl.Phys.57 (1985) 3319
19. H.de Raedt, J.Fivez and A.Lagendijk: Phys.Lett.104A (1984) 430
    H.de Raedt and A.Lagendijk: Z.Phys.B57 (1984) 209
20. E.Loh, D.J.Scalapino and P.M.Grant: Phys.Rev.B31 (1985) 4712
21. H.de Raedt and A.Lagendijk: Phys.Rev.B33 (1986) 5102
    E.Loh, D.J.Scalapino and P.M.Grant: Phys.Rev.B33 (1986) 5104
22. M.E.Fisher, M.M.Barber and D.Jasnow, Phys.Rev.A8 (1973) 1111
23. J.M.Kosterlitz and D.J.Thouless: J.Phys.C6 (1973) 1181
    J.M.Kosterlitz: J.Phys.C7 (1974) 1046
25. M.Marcu and F.-K.Schmatzer: in preparation
26. M.Marcu, J.Mueller and F.-K.Schmatzer: in preparation
27. M.Suzuki: Phys.Lett.113A (1985) 299
28. M.Marcu and J.Mueller, in preparation
29. M.Suzuki: Phys.Rev.B31 (1985) 2957
30. I thank Dr. Miyashita for teaching me this point
31. H.J.Schulz: Orsay preprint (1986)
32. T.Onogi, S.Miyashita and M.Suzuki: in preparation